

RESEARCH PAPER



Design, synthesis, and biological evaluation of arylmethylpiperidines as Kv1.5 potassium channel inhibitors

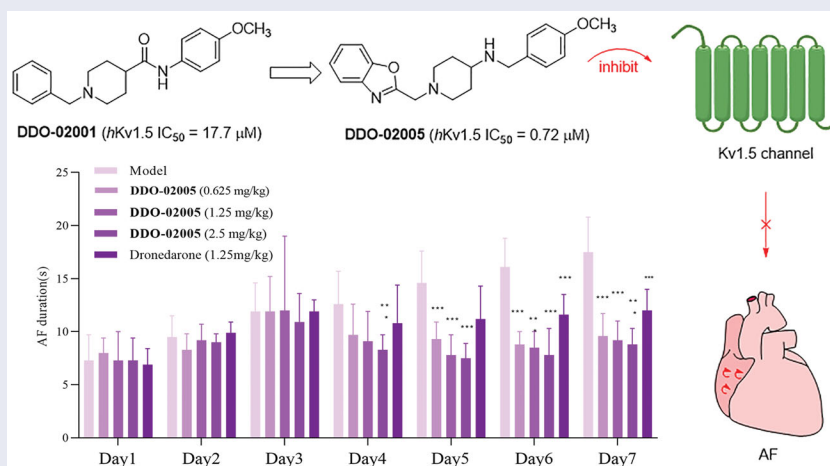
Lingyue Zhao^{a,b*}, Qian Yang^{a,b*}, Yiqun Tang^c, Qidong You^{a,b} and Xiaoke Guo^{a,b}

^aJiang Su Key Laboratory of Drug Design and Optimization, China Pharmaceutical University, Nanjing, China; ^bDepartment of Medicinal Chemistry, School of Pharmacy, China Pharmaceutical University, Nanjing, China; ^cDepartment of Clinical Pharmacy, School of Basic Medical Sciences and Clinical Pharmacy, China Pharmaceutical University, Nanjing, China

ABSTRACT

Kv1.5 potassium channel, encoded by KCNA5, is a promising target for the treatment of atrial fibrillation, one of the common arrhythmia. A new series of arylmethylpiperidines derivatives based on **DDO-02001** were synthesised and evaluated for their ability to inhibit Kv1.5 channel. Among them, compound **DDO-02005** showed good inhibitory activity ($IC_{50} = 0.72 \mu\text{M}$), preferable anti-arrhythmic effects and favoured safety. These results indicate that **DDO-02005** can be a promising Kv1.5 inhibitor for further studies.

GRAPHICAL ABSTRACT



ARTICLE HISTORY

Received 9 September 2021
Revised 9 December 2021
Accepted 9 December 2021

KEY WORDS

Kv1.5 inhibitors; atrial fibrillation; anti-arrhythmia

Introduction

Atrial fibrillation (AF) is one of the most common clinical arrhythmia with a high prevalence in general population¹, which has a close relationship with other cardiovascular diseases such as stroke, heart failure and ischaemic heart disease^{2,3}. The atria in patients with AF can develop sustained, rapid (400–600 per minute) and irregular impulsion⁴, leading to a reduced quality of life.


An important mechanism for AF is atrial electrical remodelling, which is characterised by significant shortening of atrial effective refractory period (ERP) and action potential duration (APD)^{5,6} accompanied by prolonged ventricular conduction. This pathological phenomenon is triggered by the weakening of ultra-rapid delayed rectifier potassium current (I_{Kur}) through ultra-rapid delayed rectifier potassium channel encoded by KCNA5 (Kv1.5)

gene^{7–9}, which is only expressed in atria^{10,11}. Scientists have discovered that over-expression of Kv1.5 reconstituted a 4-aminopyridine-sensitive outward K^+ current, shortened the action potential duration, eliminated early after depolarisations, shortened the QT interval, decreased dispersion of repolarisation, and increased the heart rate⁶. The underlying therapeutic principle seems clear that Kv1.5 current suppression is expected to lead to an extension in APD and increase the ERP of fibrotic atria^{12,13}.

Kv1.5 channel contains eight subunits, including four identical pore-forming α -subunits encoded by the KCNA5 gene and four accessory β -subunits (Kv β 1.2, Kv β 1.3, and Kv β 2.1) that bind to the N-terminus of the α -subunit to form $\alpha_4\beta_4$ complexes. Every α -subunit contains six transmembrane-spanning segments (S1–S6) with cytoplasmic N- and C-terminal domains (Figure 1)¹⁴. The β -subunit field received a major boost when rKv β 1.1 and rKv β 2.1 from

CONTACT Qidong You  youqd@163.com; Xiaoke Guo  kexin95@126.com  Department of Medicinal Chemistry, School of Pharmacy, China Pharmaceutical University, Nanjing 210009, China

*These authors have contributed equally to this work.

 Supplemental data for this article can be accessed [here](#).

© 2022 The Author(s). Published by Informa UK Limited, trading as Taylor & Francis Group.

This is an Open Access article distributed under the terms of the Creative Commons Attribution License (<http://creativecommons.org/licenses/by/4.0/>), which permits unrestricted use, distribution, and reproduction in any medium, provided the original work is properly cited.

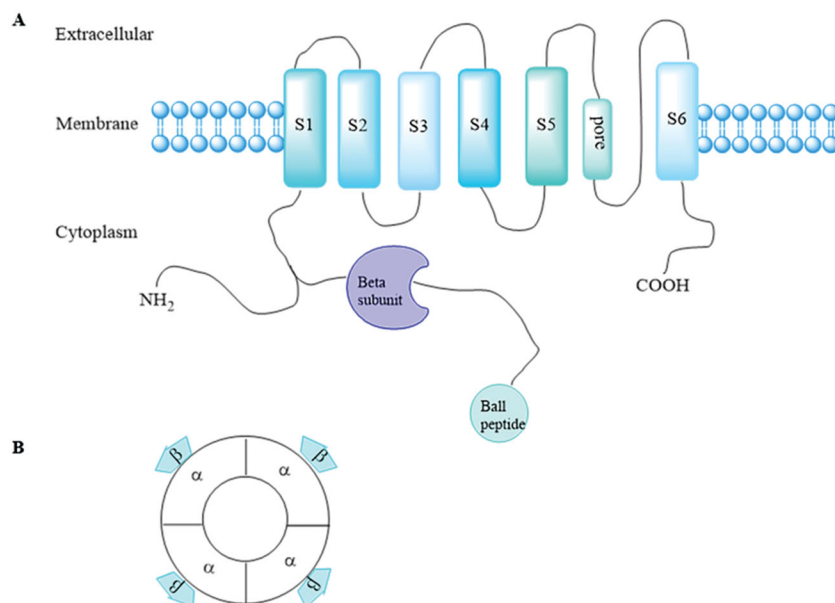


Figure 1. (A) Structure of one Kv1.5 α -subunit with six membrane-spanning domains and the intracytoplasmic accessory β -subunits. (B) α and accessory β -subunits co-assemble as tetramers to form the functional channel.

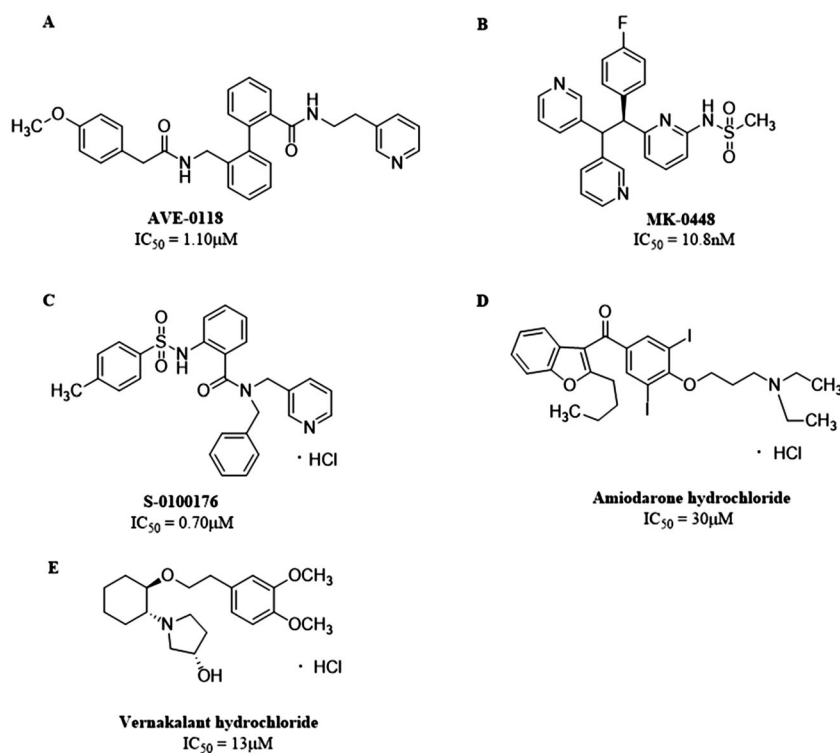


Figure 2. Structures of (A) AVE-0118. (B) MK-0448. (C) S-0100176. (D) Amiodarone hydrochloride. (E) Vernakalant hydrochloride.

ratbrain cDNA libraries were isolated by bovine amino acid sequence^{14,15}. Since then, multiple K⁺ channel β -subunit genes such as Kv β 3.1, Kv β 4.1, Kv β 1.2, Kv β 1.3 were cloned from brain and cardiac resources, respectively^{16–18}. Kv β 1.1–1.3 proteins arise by alternative splicing from the same gene¹⁷, whereas Kv β 2.1, 3.1, and 4.1 are derived from distinct genes. Though multiple K⁺ channel β subunit genes were encoded by different genes, they shared a common conserved core of over 85% amino identity, which laid a foundation for interaction with Kv α subunits. Phosphorylation of the β -subunit is important in modulation of

α/β interactions¹¹. In Kv1.5 channel, Kv1.5 α -subunits co-assembled with Kv β 1.2 subunits to form the I_{Kur} in human atrium¹⁹.

So far, two categories of Kv1.5 inhibitors have been discovered: selective inhibitors, including **AVE-0118**, **MK-0448**, **S-0100176**, etc., and non-selective inhibitors such as **Amiodarone**, **Vernakalant** and so on (Figure 2). The selectivity of I_{Kur} blockers to prolong atrial versus ventricular ERP can be explained by the presence of I_{Kur} in atria. However, in healthy non-remodeled atria, the prolongation of AERP can be related to the blockade of I_{Na+} . Most of the new drugs developed as selective I_{Kur} blockers show

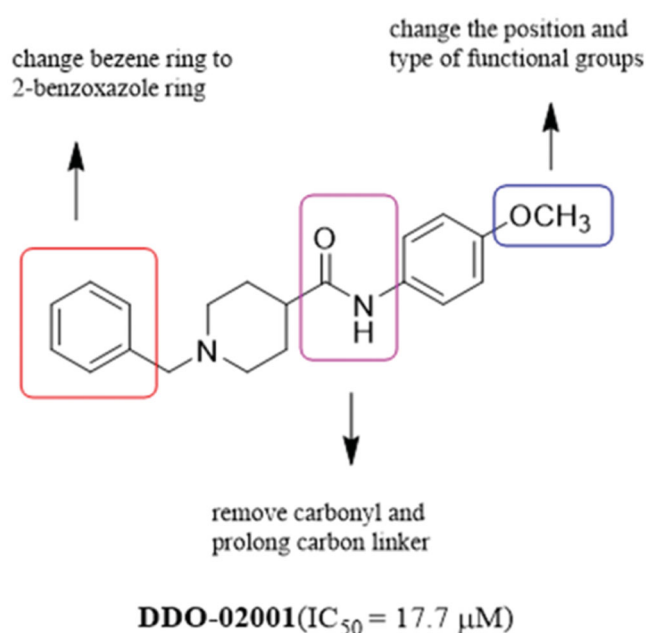


Figure 3. Structure of DDO-02001 and strategy for optimisation.

mixed ion channel activity, blocking other cardiac K^+ , Ca^{2+} and Na^+ currents, and their affinity is comparable to I_{Kur} , that is, they produce non-selectivity I_{Kur} blockade¹⁹. For instance, Vernakalant inhibits the I_{Na} and slow conduction velocity and increase diastolic threshold of excitation in atria but not in ventricles^{20–22}, and some I_{Kur} blockers such as **AVE-0118** inhibits I_{to} to prolong human APD at the plateau level²³. Therefore, drugs that affect multiple currents can be much more effective than blockers that affect only one current, as several different ionic currents contribute to human atrial AP²⁴.

In order to discover Kv1.5 inhibitors with new scaffold, an in-house compound library was screened using whole-patch clamp technique. Compound **DDO-02001** with moderate inhibitory effect on Kv1.5 channel ($IC_{50} = 17.7 \mu M$) was obtained as a lead compound. To improve the Kv1.5 inhibitory activity, a series of compounds with arylmethylpiperidines skeleton were designed (Figure 3) and synthesised, their biological activities were tested and structure-activity relationships (SAR) were discussed. Ultimately, the potent Kv1.5 channel inhibitor **DDO-02005** was acquired with acceptable therapeutic effect in atrial fibrillation model and considerable inhibitory effect on arrhythmia, herein the arrhythmia was induced by aconitine in rats.

Experimental

Chemistry

All starting materials and solvents were purchased from commercial sources and used without any additional purification. Melting points (m.p.) were detected by a Melt-Temp II apparatus. All the reactions were monitored using TLC silica gel plates (GF254, 0.25 mm) and visualised under UV light. The 1H -NMR and ^{13}C -NMR spectra were measured on a Bruker AV-300 instrument using deuterated solvents with tetramethylsilane (TMS) as internal standard. High-resolution mass spectra (HRMS) were obtained on Water Q-TOF micro mass spectrometer. The purity ($\geq 95\%$) of the target compounds was verified by High Performance Liquid Chromatography (HPLC) analysis (Agilent C18 column, 4.6×150 mm, $5 \mu m$).

Synthesis of tert-butyl 4-((4-methoxyphenyl)carbamoyl)piperidine-1-carboxylate (2)

To a solution of 1-(tert-butoxy carbonyl) piperidine-4-carboxylic acid (1.29 g, 0.01 mol) in anhydrous THF (10 ml), EDC (0.01 mol) and DMAP (0.01 mol) were added. The mixture was stirred at r.t. for 15 min. Then 4-methoxyaniline (0.011 mol) was added. The mixture was poured into water and filtered after stirring for another 1 h at r.t., then the solid was washed with water and dried under infra-red light to give white solid. (1.5 g, 45%, m.p. 154–155 °C); 1H -NMR (300 MHz, $CDCl_3$) δ 7.40 (d, $J = 9$ Hz, 2H), 7.26 (s, 1H), 6.85 (d, $J = 9$ Hz, 2H), 4.16–4.21 (m, 2H), 3.79 (s, 3H), 2.74–2.83 (m, 2H), 2.32–2.36 (m, 1H), 1.88–1.92 (m, 2H), 1.59–1.80 (m, 2H), 1.47 (s, 9H).

Synthesis of N-(4-methoxyphenyl) piperidine-4-carboxamide trifluoroacetate (3)

To a solution of tert-butyl 4-(3-methoxyphenylcarbamoyl) piperidine-1-carboxylate (3.34 g, 0.01 mol) in methanol (40 ml), trifluoroacetic acid (TFA) (1.5 ml, 0.02 mol) was added. The mixture was stirred at room temperature for 12 h and concentrated in vacuum until dryness. The solid was washed with diethyl ether and dried under infra-red light to give white solid (1.5 g, 43.1%); 1H -NMR (300 MHz, $CDCl_3$) δ 9.71 (s, 1H), 7.53–7.47 (m, 2H), 6.91–6.86 (m, 2H), 3.78 (s, 3H), 3.09 (dd, $J = 12.4, 7.1, 5.3$ Hz, 2H), 2.99 (dd, $J = 12.4, 5.4$ Hz, 2H), 3.13–3.03 (m, 2H), 3.05–2.95 (m, 2H), 1.96 (dd, $J = 12.4, 7.1$ Hz, 2H), 1.85 (dd, $J = 12.3, 7.0$ Hz, 2H).

Synthesis of 1-(benzo[d]oxazol-2-ylmethyl) piperidin-4-one (5)

To a solution of piperidin-4-one hydrochloride (3.96 g, 0.04 mol) and K_2CO_3 (5 g, 0.036 mol) in CH_3CN (80 ml), 2-(chloromethyl) benzo[d]oxazole (5.85 g, 0.035 mol) in CH_3CN (50 ml) was added. The mixture was refluxed for 4 h and filtered. The solvent was evaporated until dryness. The residue was purified by column chromatograph over silica gel (EA/PE 1:2). The pure fractions were collected, and the solvent was evaporated (4.8 g, 60%, m.p. 86–88 °C); 1H -NMR (300 MHz, $CDCl_3$) δ 7.70–7.73 (m, 1H), 7.52–7.57 (m, 1H), 7.32–7.39 (m, 2H), 4.02 (s, 2H), 2.98 (t, $J = 6$ Hz, 4H), 2.54 (t, $J = 6$ Hz, 4H).

Synthesis of 1-benzyl-N-(4-methoxyphenyl) piperidine-4-carboxamide (DDO-02001)

To a solution of **3** (1 g, 0.0028 mol) and K_2CO_3 (5 g, 0.036 mol) in acetonitrile, (bromomethyl)benzene (0.7 ml, 0.0055 mol) was added. After refluxing for 2 h, the mixture was poured into water and extracted by ethyl acetate ($20 ml \times 3$). The organic layer was then separated and dried with anhydrous sodium sulphate, filtered and concentrated. Then purified by column chromatography over silica gel (EA/PE 1:1) to provide crude product. The crude product was crystallised in ethyl acetate to give white solid (0.6 g, 66%, m.p. 157–159 °C); 1H -NMR (300 MHz, $CDCl_3$) δ 7.49–7.41 (m, 2H), 7.37 (d, $J = 4.4$ Hz, 4H), 7.16 (s, 1H), 6.89 (d, $J = 8.9$ Hz, 2H), 3.83 (s, 3H), 3.57 (s, 2H), 3.03 (d, $J = 10.9$ Hz, 2H), 2.26 (d, $J = 10.9$ Hz, 1H), 2.08 (d, $J = 11.1$ Hz, 2H), 2.02–1.83 (m, 4H). ^{13}C -NMR (75 MHz, $DMSO-d_6$) δ 168.86, 151.62, 133.61, 126.42, 124.40, 123.54, 122.35, 117.24, 109.36, 72.84, 72.41, 71.99, 58.50, 50.77, 48.33, 39.46, 24.28. HRMS (ESI): calcd for m/z $C_{20}H_{24}N_2O_2$ $[M + H]^+$ 325.19105, found 325.19184. HPLC (methanol: water = 80: 20): $t_R = 3.1$ min, 99.43%.

Synthesis of 1-(benzo[d]oxazol-2-ylmethyl)-N-(4-methoxyphenyl) piperidine-4-carboxamide (DDO-02002)

To a solution of **3** (1 g, 0.0028 mol) and K_2CO_3 (5 g, 0.036 mol) in acetonitrile, 2-(chloromethyl)benzo[d]oxazole (0.918 g, 0.0055 mol) was added, the mixture was refluxed for 2 h, poured into water, extracted by ethyl acetate, dried over Na_2SO_4 , and filtered, and the solvent was evaporated until dryness. The residue was purified by column chromatography over silica gel (EA/PE 1:1). The solvent was evaporated and the fraction was crystallised in ethyl acetate. The precipitate was filtered off and dried to give white solid (0.7 g, 68%, m.p. 190–194 °C); 1H -NMR (300 MHz, DMSO- d_6) δ 9.72 (s, 1H), 7.77 (dt, $J=7.8, 1.6$ Hz, 2H), 7.59–7.46 (m, 2H), 7.45–7.35 (m, 2H), 6.88 (d, $J=9.0$ Hz, 2H), 3.90 (s, 2H), 3.73 (s, 3H), 3.00 (d, $J=10.9$ Hz, 2H), 2.41–2.09 (m, 3H), 1.86–1.61 (m, 4H). HRMS (ESI): calcd. for m/z $C_{20}H_{24}N_2O_2$, $[M+H]^+$ 366.18122, found 366.18188. HPLC (methanol: water = 80: 20): $t_R=5.9$ min, 95.09%.

General procedure for the synthesis of DDO-02003-DDO-02009

To a solution of **5** (0.1 g, 0.434 mmol), 6–17 (0.651 mmol) in CH_2Cl_2 were added. $NaB(OAc)_3H$ (0.183 g, 0.868 mol) was added to the solution and stirred at room temperature. After the reaction, the solvent was evaporated until dryness and quenched by adding saturated NH_4Cl . Then product was extracted with CH_2Cl_2 (20 ml*3) and dry in vacuum. HCl-EA solution was added to form the hydrochloride salt, then the solid was recrystallised with EA.

The yield, melting point, analytical data, and spectral data of each compound are given below.

1-(benzo[d]oxazol-2-ylmethyl)-N-(4-methoxyphenyl) piperidin-4-amine dihydrochloride (DDO-02003). 0.067 g, 46%, white powder, m.p. >250 °C; 1H -NMR (300 MHz, D_2O) δ 7.72 (dd, $J=7.4, 1.8$ Hz, 1H), 7.50–7.37 (m, 1H), 7.50–7.37 (m, 2H), 7.29 (dd, $J=7.9, 5.4$ Hz, 2H), 7.07–7.01 (m, 2H), 4.70 (s, 2H), 3.80 (d, $J=3.9$ Hz, 1H), 3.76 (s, 3H), 3.75 (s, 2H), 3.26 (td, $J=13.2, 2.9$ Hz, 2H), 2.27 (d, $J=13.9$ Hz, 2H), 2.11–1.92 (m, 2H). HRMS (ESI) calcd. for m/z $C_{20}H_{23}N_3O_2$, $[M+H]^+$ 338.18639, found 338.1863. HPLC (methanol: water = 80: 20): $t_R=6.9$ min, 95.18%.

1-(benzo[d]oxazol-2-ylmethyl)-N-benzylpiperidin-4-amine dihydrochloride (DDO-02004). 0.058 g, 42%; white powder, m.p. > 250 °C; 1H -NMR (300 MHz, Deuterium Oxide) δ 7.75–7.68 (m, 1H), 7.65–7.59 (m, 1H), 7.43 (dd, $J=7.5, 1.5$ Hz, 2H), 7.38 (s, 5H), 4.70 (s, 2H), 4.21 (s, 2H), 3.80 (d, $J=12.8$ Hz, 2H), 3.67–3.42 (m, 1H), 3.28 (t, $J=12.9$ Hz, 2H), 2.44 (d, $J=14.0$ Hz, 2H), 2.17–1.80 (m, 2H). HRMS (ESI) calcd. for m/z $C_{20}H_{23}N_3O$, $[M+H]^+$ 322.19166, found 322.19139. HPLC (methanol: water = 80: 20): $t_R = 4.5$ min, 98.09%.

1-(benzo[d]oxazol-2-ylmethyl)-N-(4-methoxybenzyl)piperidin-4-amine dihydrochloride (DDO-02005). 0.06 g, 40%; white powder, m.p. 207–211 °C; 1H -NMR (300 MHz, Deuterium Oxide) δ 7.55 (dd, $J=18.2, 7.4$ Hz, 2H), 7.41–7.18 (m, 4H), 6.90 (d, $J=8.2$ Hz, 2H), 4.07 (s, 2H), 3.81 (s, 2H), 3.70 (s, 3H), 3.21–2.86 (m, 2H), 2.24 (t, $J=12.0$ Hz, 2H), 2.14–1.97 (m, 2H), 1.72–1.43 (m, 2H). HRMS (ESI) calcd. for m/z $C_{21}H_{25}N_3O_2$, $[M+H]^+$ 352.20108, found 352.20195. HPLC (methanol: water = 80: 20): $t_R = 4.3$ min, 95.27%.

1-(benzo[d]oxazol-2-ylmethyl)-N-(4-fluorobenzyl) piperidin-4-amine dihydrochloride (DDO-02006). 0.065 g, 44%; white powder, m.p. >250 °C; 1H -NMR (300 MHz, Methanol- d_4) δ 7.83–7.77 (m, 1H), 7.75–7.68 (m, 1H), 7.64 (dd, $J=8.5, 5.3$ Hz, 2H), 7.50 (dd, $J=8.3,$

7.1, 3.9 Hz, 2H), 7.25 (t, $J=8.6$ Hz, 2H), 4.54 (s, 2H), 4.32 (s, 2H), 3.70 (d, $J=12.1$ Hz, 2H), 3.50 (d, $J=12.3$ Hz, 1H), 3.08 (t, $J=12.0$ Hz, 2H), 2.44 (d, $J=13.2$ Hz, 2H), 2.19–2.04 (m, 2H). HRMS (ESI) calcd. for m/z $C_{20}H_{22}FN_3O$, $[M+H]^+$ 340.18197, found 340.18205. HPLC (methanol: water = 80: 20): $t_R = 11$ min, 96.98%.

1-(benzo[d]oxazol-2-ylmethyl)-N-(2-methoxybenzyl)piperidin-4-amine dihydrochloride (DDO-02007). 0.068 g, 45%; white powder, m.p. >250 °C; 1H -NMR (300 MHz, Deuterium Oxide) δ 7.77–7.70 (m, 1H), 7.68–7.62 (m, 1H), 7.52–7.35 (m, 3H), 7.31 (dd, $J=7.5, 1.7$ Hz, 1H), 7.09–6.92 (m, 2H), 4.71 (s, 2H), 4.24 (s, 2H), 3.82 (s, 5H), 3.62–3.47 (m, 1H), 3.30 (dd, $J=13.8, 11.0$ Hz, 2H), 2.45 (d, $J=14.0$ Hz, 2H), 2.11–1.90 (m, 2H). HRMS (ESI) calcd. for m/z $C_{21}H_{25}N_3O_2$, $[M+H]^+$ 352.20329, found 352.20195. HPLC (methanol: water = 80: 20): $t_R = 6.13$ min, 96.50%.

1-(benzo[d]oxazol-2-ylmethyl)-N-(4-methylbenzyl)piperidin-4-amine dihydrochloride (DDO-02008). 0.070 g, 48%; white powder, m.p. 205–207 °C; 1H -NMR (300 MHz, Methanol- d_4) δ 7.77–7.71 (m, 1H), 7.69–7.61 (m, 1H), 7.50–7.42 (m, 2H), 7.39 (d, $J=7.9$ Hz, 2H), 7.29 (d, $J=7.7$ Hz, 2H), 4.14 (s, 2H), 3.97 (s, 2H), 3.16 (d, $J=12.3$ Hz, 2H), 3.10–3.01 (m, 1H), 2.36 (d, $J=11.2$ Hz, 2H), 2.17 (d, $J=12.3$ Hz, 2H), 1.95 (s, 3H), 1.86–1.69 (m, 2H). HRMS (ESI) calcd. for m/z $C_{21}H_{25}N_3O$, $[M+H]^+$ 336.20704, found 336.20686. HPLC (methanol: water = 80: 20): $t_R=5.74$ min, 95.79%.

1-(benzo[d]oxazol-2-ylmethyl)-N-phenethylpiperidin-4-amine hydrochloride (DDO-02009). 0.067 g, 46%; white powder, m.p. >250 °C; 1H -NMR (300 MHz, Deuterium Oxide) δ 7.74 (d, $J=7.6$ Hz, 1H), 7.65 (d, $J=7.9$ Hz, 1H), 7.52–7.38 (m, 2H), 7.30 (dt, $J=20.8, 7.6$ Hz, 5H), 4.70 (s, 2H), 3.79 (d, $J=13.0$ Hz, 2H), 3.51 (td, $J=11.9, 6.0$ Hz, 1H), 3.38–3.17 (m, 4H), 2.96 (t, $J=7.6$ Hz, 2H), 2.38 (d, $J=14.0$ Hz, 2H), 2.01–1.89 (m, 2H). HRMS (ESI) calcd. for m/z $C_{21}H_{25}N_3O$, $[M+H]^+$ 336.20704, found 336.20692. HPLC (methanol: water = 80: 20): $t_R=6.58$ min, 95.24%.

Biological evaluation

Whole-patch clamp assay

The HEK 293 cell line that stably expressed *hKv1.5* potassium channel was a kind gift from Dr. Gui-Rong Li (Department of Medicine and Department of Physiology, Li Ka Shing Faculty of Medicine, The University of Hong Kong, Pokfulam, Hong Kong, SAR, China). Transfected HEK 293 cells were maintained at 37 °C in Minimal Eagle Medium (MEM) or Dulbecco's Modified Eagle Medium (DMEM) supplemented with 10% foetal bovine serum, 1% penicillin-streptomycin, 2 mmol/L L-glutamine, 0.1 mmol/L non-essential amino acids, 1 mmol/L sodium pyruvate, and 0.2 mg/mL geneticin (Invitrogen Corporation, Carlsbad, CA, USA). Cells were passaged weekly and used at $\leq 80\%$ confluence. For electrophysiological recordings, the cells were harvested from the culture dish by trypsinisation, and then washed twice with standard MEM or DMEM and maintained in culture medium at room temperature for later use on the same day.

The whole-cell membrane currents were recorded by the patch-clamp technique, using an EPC-10 double patch-clamp amplifier (HEKA, Pfalz, Germany). Recording pipettes, made from borosilicate glass (1.2 mm, o.d.), pulled with a pipette puller (PIP5, HEKA, Germany), had resistances of between 4 and 6 Ω when filled with the pipette solution. After a giga-seal ($>10 G\Omega$) was obtained, the cell membrane was ruptured by gentle suction to

establish the whole-cell configuration. The series resistance was electrically compensated to minimise the capacitive surge on the current recording. Peak current amplitude was determined after baseline correction. Pulse software (HEKA, Pfalz, Germany) was used to generate voltage pulse protocols and to record and analyse data. Compounds were applied at least 5 min after current stabilisation. The data are presented as the mean and standard deviation (mean \pm SD). The differences between control levels and the changes caused by the compound application were tested using Student's *t*-test. A value of $p < 0.05$ was considered statistically significant. All experiments were performed at 25 °C.

CaCl₂-ACh induced AF model

SD rats (250 \pm 20 g) were raised in an environment with a temperature of 20–24 °C and a humidity of 50%, and lighting for 12 h, drink and eat freely, and then anaesthetised with 10% chloral hydrate (Sinopharm Chemical Reagent Co., Ltd, Shanghai, China) (3 ml/kg, i.p.), followed by i.v. administration of CaCl₂ (10 mg/mL) and acetylcholine (ACh; 66 mg/mL) through the caudal vein (1 ml/kg) once a day for 7 days. A typical AF electrocardiogram (ECG) appeared immediately and recovered to sinus rhythm in the following 10 s. The ECG was recorded for the complete experiment procedure from rat anaesthetisation to the ECG being restored to normal, approximately 50 min for each rat each day (i.e. from Day 1 to Day 7).

On Day 4, rats were randomly divided into five groups ($n = 10$ /group): (1) AF model group: repeated prior procedure until day 7, CaCl₂ (10 mg/mL, i.v.) and ACh (66 mg/mL, i.v.); (2) (3) and (4) **DDO-02005** treatment groups: **DDO-02005** (0.625 mg/kg and 1.25 mg/kg, 2.5 mg/kg, i.p.) combined with CaCl₂ (10 mg/mL) and ACh (66 mg/mL) (i.v.) from Day 4 to Day 7; (5) dronedarone treatment group: dronedarone (1.25 mg/kg, i.p.) combined with CaCl₂ (10 mg/mL) and ACh (66 mg/mL) (i.v.) from Day 4 to Day 7. Controls were anaesthetised with 10% chloral hydrate (3 ml/kg, i.p.), followed by physiological saline i.v. for 7 days.

The disappearance of the P wave and appearance of the f wave was determined as the beginning of AF while the end was designated by disappearance of the f wave and the appearance of the regular P wave, e.g., sinus rhythm recovery. Other ECG parameters including heart rate (HR), PR, QRS, and rate-corrected QT_c interval ($QT_{cd} = QT/(R-R)^{1/2}$) were also recorded as this study was focussed on HR and rate-corrected QT_c interval analysis.

Aconitine induced arrhythmia model

SD rats (250 \pm 20 g) were anaesthetised and the jugular vein was surgically separated. After intubation, rats in each group were given intravenous normal saline (model group), each dose of the compound (0.1 mg/kg, 1 mg/kg, 3 mg/kg, 9 mg/kg). 5 min after administration, the jugular vein was given aconitine at a constant rate (0.20–0.22 ml/min, 1 μ g/ml).

The experiment uses the BL-420F biological function test system (Chengdu Taimeng Technology Co., Ltd.) to continuously record the changes of the electrocardiogram of the rats before and after the administration (lead II), and calculate the amount of aconitine injected (μ g/100g) when the rats have premature ventricular beats (VP).

Pharmacokinetics studies

12 beagle dogs (male and female) were taken, randomly divided into two groups equally. The experimental animals were fasted overnight (more than 10 h) 12 h before the experiment. The drug was administered at 7:00 am the next day at a dose of 1 mg/kg by intravenous injection and 1.25 mg/kg by oral administration. The drug was dissolved in 100 ml normal saline and administered by gavage. 3 ml of blood was collected from the vein before gavage (0 min) and 10, 20, 30, 45 min, 1, 1.5, 2, 3, 4, 6, 8, 10, 12 h. After gavage, the plasma was collected and stored at –20 °C for the detection of blood drug concentration, and the accurate time of blood collection was recorded in detail. The test dogs were fasted overnight (more than 10 h) before taking the medicine, and the corresponding preparations were given on an empty stomach at 8:30 the next morning. Blood was collected according to the design time point, put into a test tube, stood for half an hour, centrifuged at 3500 rpm for 15 min, supernatant was taken into a centrifuge tube, frozen at –20 °C for 1 week, and the washout period of cross-medication was 1 week.

Safety studies

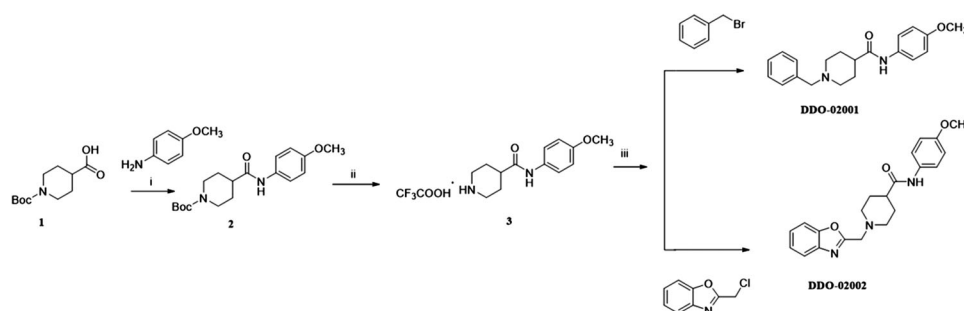
The healthy, male guinea pigs weighing 250–300 g were anaesthetised with urethane and fixed on the operating table. Using needle electrodes to pierce the extremities and subcutaneously on the chest, and the whole heart lead electrocardiogram was recorded. The right jugular vein is separated and cannulated. After 5 min, **DDO-02005**, Azimilide, (3×10^{-7} , 10^{-6} , 3×10^{-6} , 10^{-5} , 3×10^{-5} mol/kg) dissolved in saline were given cumulative injections, each concentration is given in equal volume (1.5 ml/kg). After administration, the BL-420F biological function experiment system recorded synchronous body surface electrocardiogram (adjust control parameter gain G: 1mv, time constant T: 0.1 s, low channel filter 100 Hz, scanning speed 250 ms/div, and start 50 Hz suppression).

ECG analysis: To observe the effects of compounds on the heart rate and QT interval of animal standard II lead ECG. Measure the cardiac cycle of each lead. Each lead continuously measured 6 complete cardiac cycles, and the average value was taken as the QT interval of that lead. The QT interval is measured from the beginning of the QRS wave to the end of the T wave. When the T wave is flat or there is a U wave, the method for judging the end of the T wave is: (1) the intersection of the T wave and the equipotential line; (2) the notch between the T wave and the U wave; (3) the intersection point of the T wave descending notch and the equipotential line; if the T wave is low and it is difficult to determine the end point, the lead is discarded. QT_d is the difference between the maximum and minimum QT interval in the measured 12 leads, and the calculation formula is $QT_d = QT_{max} - QT_{min}$. Considering that the QT interval is affected by the heart rate, the Bazett formula is used for heart rate correction to calculate the QT_{cd} after the heart rate correction. The calculation formula is $QT_{cd} = QT/(R-R)^{1/2}$, and the R–R in the formula refers to the R–R interval period. All measurement work is manually measured by the experimenter.

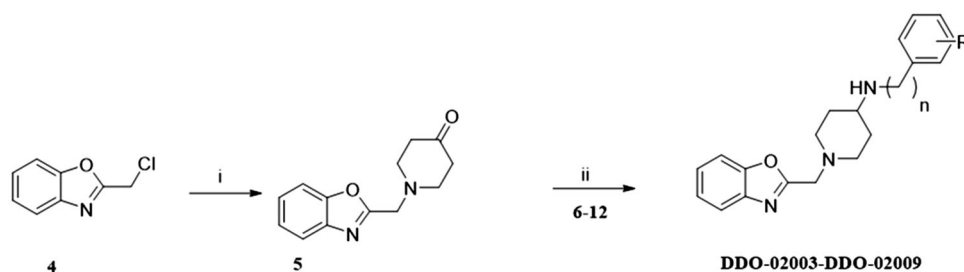
Result and discussion

Chemistry

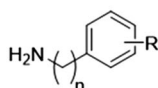
To improve the Kv1.5 inhibitory activity, we changed the aromatic ring, linker and substituent of **DDO-02001** as shown in Figure 2. As shown in Scheme 1, 1-(tert-butoxycarbonyl)piperidine-4-carboxylic



Scheme 1. Synthesis of **DDO-02001** and **DDO-02002**. Reagents and conditions: (i) EDCI, DMAP, THF, r.t.; (ii) CF_3COOH , DMF, r.t.; (iii) K_2CO_3 , CH_3CN , 80°C , reflux.



Structure of **6-12**



n	R	n	R		
6	0	4-OCH ₃	10	1	2-OCH ₃
7	1	H	11	1	4-CH ₃
8	1	4-OCH ₃	12	2	H
9	1	4-F			

Scheme 2. Synthesis of **DDO-02003-02009**. Reagents and conditions: (i) piperidin-4-one-hydrochloride, K_2CO_3 , r.t.; (ii) $\text{NaB}(\text{OAc})_3\text{H}$, anhydrous. $\text{ClCH}_2\text{CH}_2\text{Cl}$, r.t.

acid (**1**) was reacted with 4-methoxy-aniline, EDCI and DMAP to get **2**, which was then treated with trifluoroacetic acid (TFA) and dichloromethane mixture at room temperature to get secondary amine **3**. **3** was treated with benzyl bromide or 2-(chloromethyl)-benzo[d]oxazole in the presence of K_2CO_3 to afford **DDO-02001** and **DDO-02002**. Intermediate **5** was synthesised from the reaction of **4** and piperidin-4-one hydrochloride. Treatment of **5** and a series of amine compounds with $\text{NaB}(\text{OAc})_3\text{H}$ gave **DDO-02003 ~ DDO-02009** as described in [Scheme 2](#).

Structure-activity relationship studies of arylmethylpiperidines derivatives

In order to investigate the SAR (Structure-activity Relationship), whole-cell patch clamp technique was applied to analyse the inhibitory activities of Kv1.5 channel of target compounds. Results are listed in [Table 1](#).

By comparing the biological results of compounds **DDO-02001** and **DDO-02002**, it can be seen that replacing the benzene ring of molecule **DDO-02001** with a benzoxazole ring improved the biological activity (**DDO-02001** $\text{IC}_{50} = 17.7\ \mu\text{M}$ vs. **DDO-02002** $\text{IC}_{50} = 8.96\ \mu\text{M}$). Carbonyl is not so important, because the removal of carbonyl lead to the promotion of inhibition effect proved by **DDO-02002** and **DDO-02003** ($\text{IC}_{50} = 1.57\ \mu\text{M}$). Replacing the linker L from $-\text{NH}-$ to $-\text{NH}-\text{CH}_2-$ slightly increased the activity (**DDO-02003** vs. **DDO-02005**); Extending the carbon

Table 1. Inhibition activities of **DDO-02002-02009** on Kv1.5 channel

Comp.	L	R	$h\text{Kv}1.5\ \text{IC}_{50}\ (\mu\text{M})$
DDO-02002	$-\text{CONH}-$	4-OCH ₃	8.96 ± 1.15
DDO-02003	$-\text{NH}-$	4-OCH ₃	1.57 ± 0.26
DDO-02004	$-\text{NH}-\text{CH}_2-$	H	0.95 ± 0.13
DDO-02005	$-\text{NH}-\text{CH}_2-$	4-OCH ₃	0.72 ± 0.08
DDO-02006	$-\text{NH}-\text{CH}_2-$	4-F	3.24 ± 0.29
DDO-02007	$-\text{NH}-\text{CH}_2-$	2-OCH ₃	>20
DDO-02008	$-\text{NH}-\text{CH}_2-$	4-CH ₃	>20
DDO-02009	$-\text{NH}-\text{CH}_2-\text{CH}_2-$	H	>20
DDO-02001			17.71 ± 2.93

chain to $-\text{NH}-\text{CH}_2-\text{CH}_2-$, the activity decreased (**DDO-02004** vs **DDO-02009**), suggesting the linker $-\text{NH}-\text{CH}_2-$ was the best choice. Different substituents on the benzene ring were changed to discuss their influence on the effect of the compound. Compared with **DDO-02005**, **DDO-02006** with electron

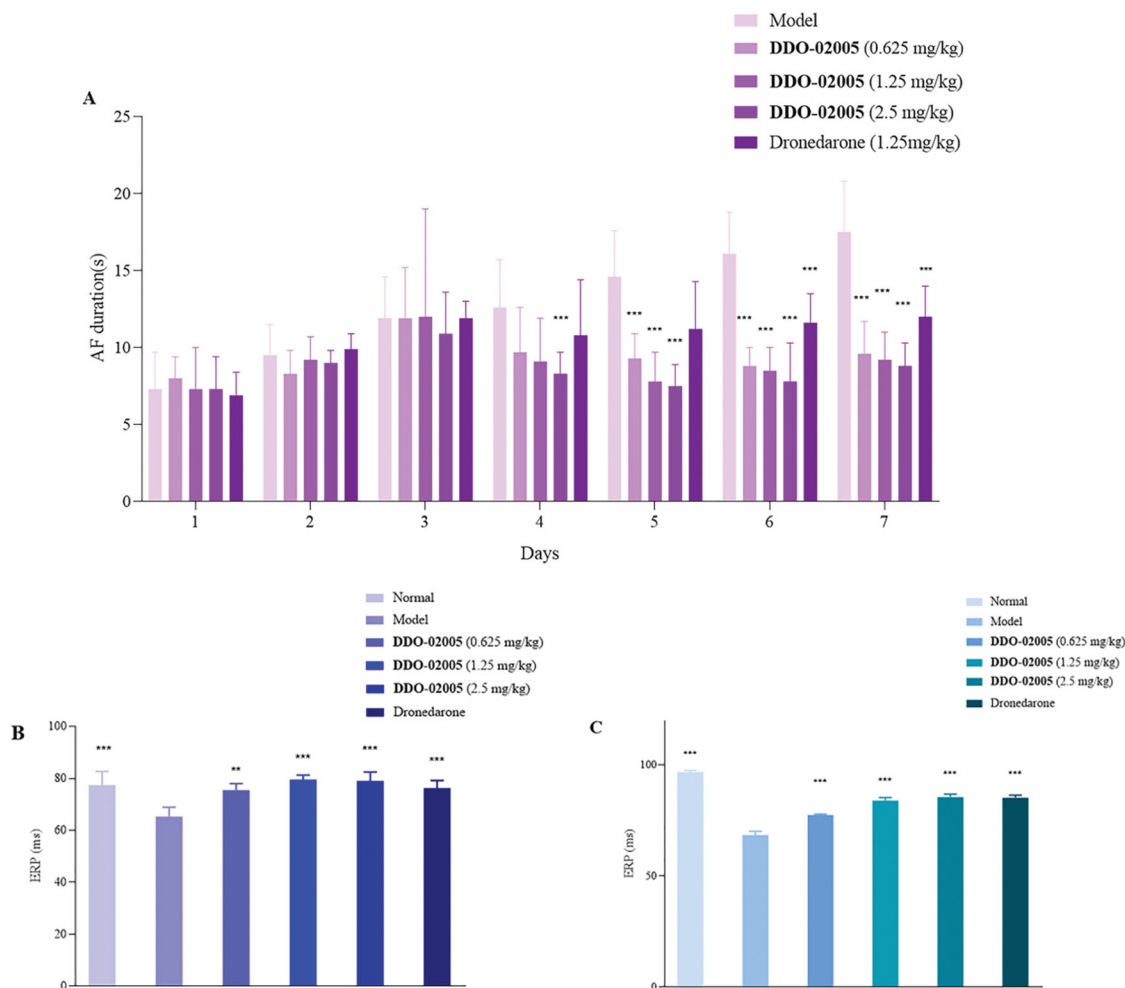


Figure 4. Effect of compound DDO-02005 and dronedarone on (A) atrial fibrillation, (B) atrial ERP and (C) ventricle ERP. Values of $*p < 0.05$, $**p < 0.01$ and $***p < 0.001$ were considered statistically significant.

withdrawing group on the benzene ring has a decreased inhibition rate of Kv1.5 channel ($IC_{50} = 3.24 \mu M$), implying that methoxyl group might be a preferred option to improve the inhibitory activity. Changing the position and type of the electron donating group in **DDO-02005** to get **DDO-02007** and **DDO-02008**, the activity decreased, suggesting that para-methoxy substitution is the best choice to exert inhibitory activity.

Through the above comparison, we screened out the best compound **DDO-02005**, and a series of subsequent experiments were conducted to verify its pharmacodynamic and pharmacokinetic properties.

Effect of DDO-02005 on AF model induced by $CaCl_2$ -ACh

A classic pathological model of atrial fibrillation induced by calcium chloride-acetylcholine ($CaCl_2$ -ACh) in rats was applied to evaluate the therapeutic effect of the active compound **DDO-02005** on atrial arrhythmia as described previously²⁵, dronedarone was selected as a positive control. The results were characterised by the changes of atrial fibrillation duration, atrial ERP (AERP) and ventricle ERP (VERP) before and after treatment with **DDO-02005**.

The results showed that during Day1 – Day3 (model-creation), there was no significant difference between model group and treatment groups. The durations of AF in rats treated with **DDO-02005** (from Day 4 to Day 7) were shortened significantly. Starting from the fifth day, the effect of **DDO-02005** on the

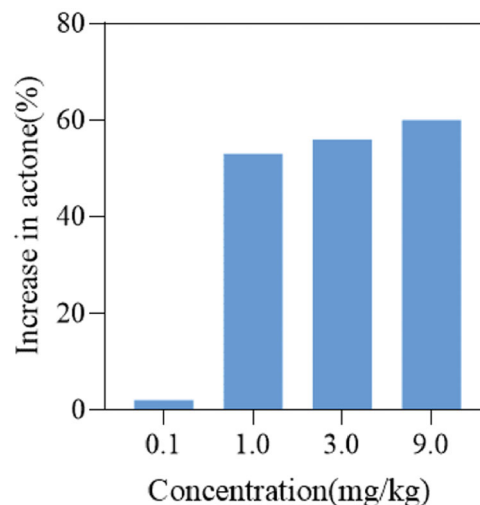


Figure 5. DDO-02005 inhibits the arrhythmia induced by aconitine in rats.

shortening of atrial fibrillation time showed a significant concentration-response relationship. As shown in Figure 4(B,C), the AERP and VERP of AF rats treated with **DDO-02005** were increased to normal level, respectively, at the dose of 2.5 mg/kg. It's worth noting that the AF therapeutic effect of **DDO-02005** is better than that of dronedarone.

Effect of DDO-02005 on rat arrhythmia induced by aconitines

Aconitine is a neurotoxin with strong cardiotoxicity^{26,27} which can promote the opening of L-type calcium channels on rat ventricular myocyte membranes, increase calcium influx, cause cytoplasmic calcium overload, and lead to arrhythmia^{9,28}.

To verify the effect of **DDO-02005** on arrhythmia inhibition, we established an aconitine-induced arrhythmia model in 30 rats as previously described²⁹. After intubation, rats in each group

were given intravenous physiological saline, and four different concentrations (0.1, 1, 3, and 9 mg/kg) of **DDO-02005** (treatment group). Taking the concentration of aconitine required to cause atrial fibrillation in the model group as a control, the concentration of aconitine increased by 2, 53, 56, and 60%, respectively. The results turned out that the compound **DDO-02005** can effectively combat the arrhythmogenic toxicity of aconitine (Figure 5).

Table 2. Pharmacokinetic parameters regarding lead compound **DDO-02005** (mean \pm SD, $n = 6$)

Parameter	<i>i.v.</i>	<i>p.o.</i>
Dose (mg/kg)	1.00	1.25
$t_{1/2}$ (h)	3.23 ± 1.07	6.25 ± 2.40
C_{max} ($\mu\text{g/L}$)	90.23 ± 28.83	1.27 ± 0.40
$AUC_{(0-t)}$ ($\mu\text{g/L}\cdot\text{h}$)	178.42 ± 39.33	4.41 ± 0.69
CL (L/h/kg)	5.83 ± 1.44	36.51 ± 2.54

Pharmacokinetic (PK) study of DDO-02005

Single-dose PK studies were then performed with beagle dogs at 1 mg/kg by intravenous injection (*i.v.*) and 1.25 mg/kg by oral administration (*p.o.*), the results were summarised in Table 2. **DDO-02005** achieved the maximum plasma concentration (C_{max}) of 1.274 $\mu\text{g/L}$, the elimination half-life ($t_{1/2}$) of 6.245 h. In addition, **DDO-02005** showed a plasma clearance (CL) of 5.834 L/h/kg after

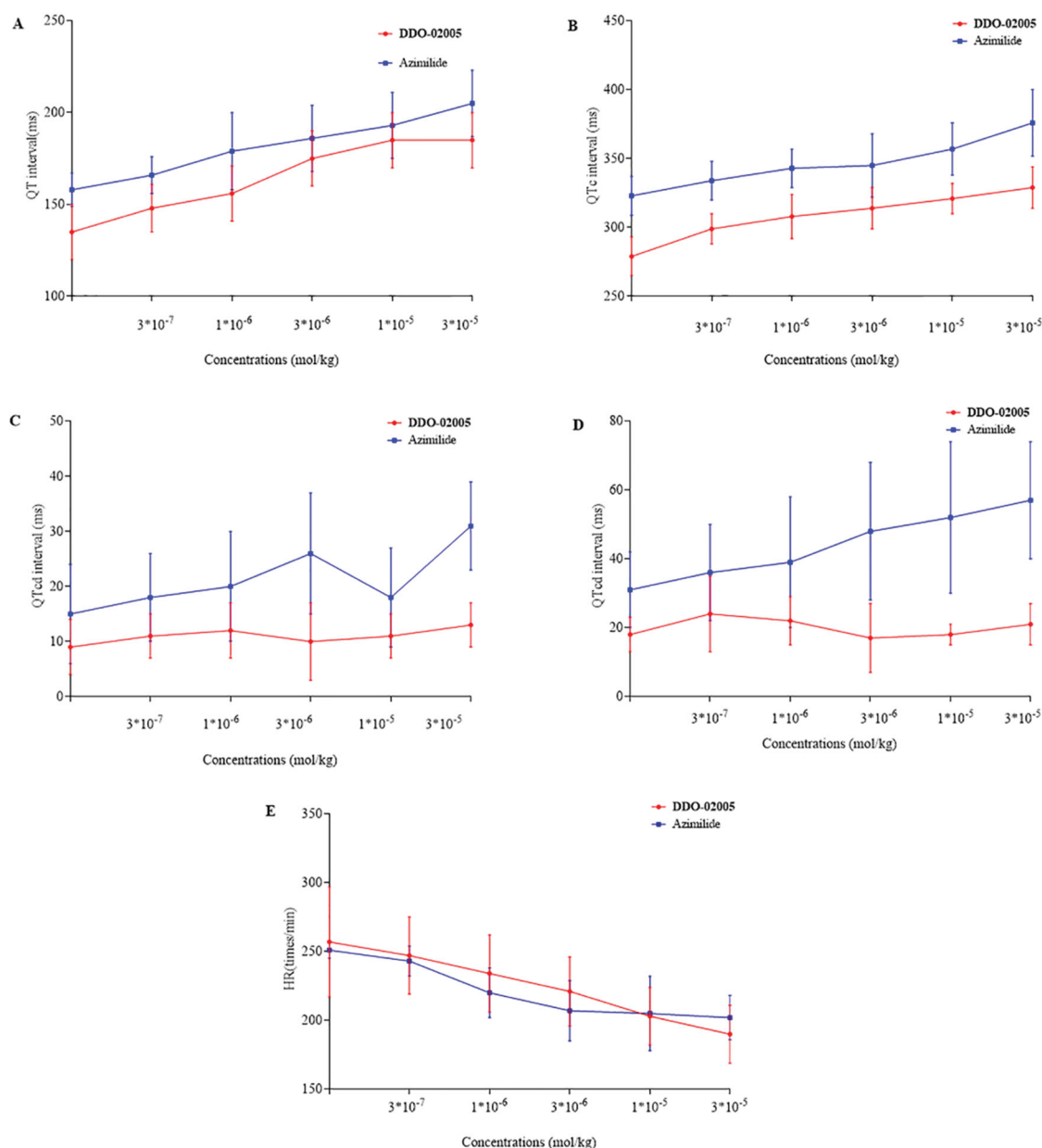


Figure 6. Cardiovascular parameters of guinea pigs after treated with compound **DDO-02005** (red) and Azimilide (blue), (A) QT interval. (B) QT_c interval. (C) QT_d interval. (D) QT_{cd} interval. (E) heart rate (HR). The values shown are the mean \pm SD ($n = 6$).

the intravenous injection. Overall, the pharmacokinetic properties of **DDO-02005** need to be further optimised.

Preliminary safety evaluation of DDO-02005

We used a 12-lead electrocardiogram to compare preliminary safety between compound **DDO-02005** and Azimilide. As shown in Figure 6, though there were no statistically significant differences between **DDO-02005** and Azimilide in prolonging QT interval (Figure 6(A)), QT_c interval (Figure 6(B)), and heart rate (Figure 6(E)), **DDO-02005** had less effect on QT dispersion (Figure 6(C)) and QT_{cd} (Figure 6(D)) on guinea pigs. The heart rate of guinea pigs slowed down obviously when **DDO-02005** was used, suggesting that it is less likely to cause arrhythmia than Azimilide. All of these figures determined that **DDO-02005** is safer than Azimilide.

Conclusion

In this study, we designed and synthesised a series of arylmethylpiperidines derivatives modified by **DDO-02001**, most of which showed effectively Kv1.5 inhibitory activities. Especially, **DDO-02005** showed excellent inhibition effect of Kv1.5 with IC₅₀ of 0.72 μM. It displayed good anti-AF effect in CaCl₂-ACh AF model and effective anti-arrhythmic activity caused by aconitine. The preliminary safety of compound **DDO-02005** was better than Azimilide showed by 12-lead electrocardiogram.

Overall, the most potent compound **DDO-02005**, which prominently inhibited Kv1.5 channel and alleviated symptom of arrhythmia with good bioavailability, in addition to being worthy of further pharmacological investigation, may be considered as a lead compound for further optimisation of Kv1.5 channel inhibitors.

Disclosure statement

No potential conflict of interest was reported by the author(s).

Funding

We are thankful for the financial support of the National Natural Science Foundation of China [grant number 81872799], [grant number 81930100], [grant number 81773639]; the Natural Science Foundation of Jiangsu Province of China [grant number BK20191321]; Fundamental Research Funds for the Central Universities [grant number 2632018ZD14]; the National Science & Technology Major Project "Key New Drug Creation and Manufacturing Program" of China [grant number 2018ZX09711002]; the Double First Class Innovation Team of China Pharmaceutical University [grant number CPU2018GY02]; the Program for Outstanding Scientific and Technological Innovation Team of Jiangsu Higher Education; the Open Project of State Key Laboratory of Natural Medicines [grant number SKLNMZZCX201803]; the Priority Academic Program Development of Jiangsu Higher Education Institutions; and the Natural Science Research Project of Jiangsu Higher Education [grant number 20KJB350001].

References

- Burashnikov A, Antzelevitch C. Can inhibition of I_{Kur} promote atrial fibrillation? *Heart Rhythm* 2008;5:1304–9.
- Mulder BA, Schnabel RB, Rienstra M. Predicting the future in patients with atrial fibrillation: who develops heart failure? *Eur J Heart Fail* 2013;15:366–7.
- Nattel S, Carlsson L. Innovative approaches to anti-arrhythmic drug therapy. *Nat Rev Drug Discov* 2006;5:1034–49.
- Wolf PA, Mitchell JB, Baker CS, et al. Impact of atrial fibrillation on mortality, stroke, and medical costs. *Arch Intern Med* 1998;158:229–34.
- Brandt MC, Priebe L, Bohle T, et al. The ultrarapid and the transient outward K⁺ current in human atrial fibrillation. Their possible role in postoperative atrial fibrillation. *J Mol Cell Cardiol* 2000;32:1885–96.
- Brunner M, Kodirov SA, Mitchell GF, et al. In vivo gene transfer of Kv1.5 normalizes action potential duration and shortens QT interval in mice with long QT phenotype. *AM J Physiol Heart Circ Physiol* 2003;285:H194–H203.
- Yang Y, Li J, Lin X, et al. Novel KCNA5 loss-of-function mutations responsible for atrial fibrillation. *J Hum Genet* 2009;54:277–83.
- Olson TM, Alekseev AE, Liu XK, et al. Kv1.5 channelopathy due to KCNA5 loss-of-function mutation causes human atrial fibrillation. *Hum Mol Genet* 2006;15:2185–91.
- Wang YJ, Chen BS, Lin MW, et al. Time-dependent block of ultrarapid-delayed rectifier K⁺ currents by aconitine, a potent cardiotoxin, in heart-derived H9c2 myoblasts and in neonatal rat ventricular myocytes. *Toxicol Sci* 2008;106:454–63.
- Nerbonne JM, Kass RS. Molecular physiology of cardiac repolarization. *Physiol Rev* 2005;85:1205–53.
- Martens JR, Kwak YG, Tamkun MM. Modulation of Kv channel alpha/beta subunit interactions. *Trends Cardiovasc Med* 1999;9:253–8.
- Tanabe Y, Hatada K, Naito N, et al. Over-expression of Kv1.5 in rat cardiomyocytes extremely shortens the duration of the action potential and causes rapid excitation. *Biochem Biophys Res Commun* 2006;345:1116–21.
- Wu SD, Fluxe A, Sheffer J, et al. Discovery and *in vitro/in vivo* studies of tetrazole derivatives as Kv1.5 blockers. *Bioorg Med Chem Lett* 2006;16:6213–8.
- Griffin A, Scott RH. Properties of K⁺ currents recorded from cultured ovine trachea submucosal gland-cells. *Resp Physiol* 1994;96:297–309.
- Rettig J, Heinemann SH, Wunder F, et al. Inactivation properties of voltage-gated K⁺ channels altered by presence of beta-subunit. *Nature* 1994;369:289–94.
- Starkus JG, Schlieff T, Rayner MD, Heinemann SH. Unilateral exposure of Shaker B potassium channels to hyperosmolar solutions. *Biophys J* 1995;69:860–72.
- England SK, Uebele VN, Kodali J, et al. A Novel K⁺ Channel beta-subunit (hKv beta 1.3) is produced via alternative mRNA splicing. *J Biol Chem* 1995;270:28531–4.
- England SK, Uebele VN, Shear H, et al. Characterization of a voltage-gated K⁺ channel beta subunit expressed in human heart. *Proc Natl Acad Sci USA* 1995;92:6309–13.
- Tamargo J, Caballero R, Gómez R, Delpón E. I(Kur)/Kv1.5 channel blockers for the treatment of atrial fibrillation. *Expert Opin Investig Drugs* 2009;18:399–416.
- Fedida D. Vernakalant (RSD1235): a novel, atrial-selective antifibrillatory agent. *Expert Opin Investig Drugs* 2007;16:519–32.
- Wettwer E, Hála O, Christ T, et al. Role of I_{Kur} in controlling action potential shape and contractility in the human atrium

- influence of chronic atrial fibrillation. *Circulation* 2004;110:2299–306.
22. Fedida D, Orth PMR, Chen JYC, et al. The mechanism of atrial antiarrhythmic action of RSD1235. *J Cardiovasc Electrophysiol* 2005;16:1227–38.
 23. Fedida D, Eldstrom J, Hesketh JC, et al. Kv1.5 is an important component of repolarizing K⁺ current in canine atrial myocytes. *Circ Res* 2003;93:744–51.
 24. Brendel J, Peukert S. Blockers of the Kv1.5 channel for the treatment of atrial arrhythmias. *Expert Opin Ther Pat* 2002;12:1589–98.
 25. Guo X, Chen CL, Yang Q, et al. Effects of a novel class III antiarrhythmic agent, CPUY11018, on rat atrial fibrillation. *Drug Develop Res* 2010;71:303–12.
 26. Chodoeva A, Bosc JJ, Guillon J, et al. 8-O-Azeloyl-14-benzoylaconine: a new alkaloid from the roots of *Aconitum karacolicum* Rapcs and its antiproliferative activities. *Bioorg Med Chem* 2005;13:6493–501.
 27. Tai YT, But PPH, Young K, Lau CP. Cardiotoxicity after accidental herb-induced aconite poisoning. *Lancet* 1992;340:1254–6.
 28. Fu M, Li RX, Fan L, et al. Sarcoplasmic reticulum Ca²⁺ release channel ryanodine receptor (RyR2) plays a crucial role in aconitine-induced arrhythmias. *Biochem Pharmacol* 2008;75:2147–56.
 29. Bartosova L, Novak F, Bebarova M, et al. Antiarrhythmic effect of newly synthesized compound 44Bu on model of aconitine-induced arrhythmia – compared to lidocaine. *Eur J Pharmacol* 2007;575:127–33.